PROCEEDINGS OF SCIENCE

Neutron Bursts from Air Showers in Ice: Implications for Neutron Detection with the South Pole Neutron Monitors

Chloe Heifner,[a,*] **Waraporn Nuntiyakul,**[b] **Andrew Puyleart**[a] **and Surujhdeo Seunarine**[a]

[a]*University of Wisconsin-River Falls, 410 S 3rd Street, River Falls, WI 54022, USA*

[b]*Department of Physics and Materials Science, Faculty of Science, Chiang Mai University, Chiang Mai, 50200, Thailand*

E-mail: chloe.heifner@my.uwrf.edu, w.nuntiyakul@gmail.com, ajpuylea@gmail.com, surujhdeo.seunarine@uwrf.edu

Observations of apparent neutron bursts from air shower cores interacting in soil have been recently reported. The primary mechanism for neutron bursts, which show up as anomalous long-duration counts in a detector, is the production of evaporation neutrons from air shower cores that enter the ground in the vicinity of a detector. Neutron monitors are ground-based detectors that observe the primary cosmic ray flux in the GeV range, allowing them to be sensitive to neutron bursts. Neutron bursts could produce an unwanted background that should be taken into account in spectral studies using neutron multiplicity. We report on a simulation study of neutron bursts from air shower cores interacting in ice and discuss the implications for spectral studies done with the South Pole Neutron Monitor. We use FLUKA, including a detailed simulation of the atmosphere, ice, and neutron monitors at the South Pole.

38th International Cosmic Ray Conference (ICRC2023)
26 July - 3 August, 2023
Nagoya, Japan

*Speaker

1. Introduction

Cosmic rays are highly energetic particles that arrive at earth from outside our solar system[1]. They span a vast range of energies, from 10^6 eV to 10^{20} eV, with a flux that decreases roughly as a power law. The flux falls even faster around 10^{15} eV, the so-called "knee" of the spectrum, where it is thought that the galactic to extra-galactic components separate. Beyond 10^{18} eV, the "ankle" of the spectrum, the flux becomes harder. Above 10^{14} eV the flux is too low for any useful observation of primary particles. However, as these primary particles enter the upper atmosphere they collide with nuclei, producing showers of secondary particles[2]. Some of these secondary particles then reach the ground where they can be observed using ground-based detectors. At the lower energy range of ground-based observations, detectors extending a few tens of square meters are sufficient for measurement of cosmic ray rates and for spectral studies.

A neutron monitor is a type of ground-based detector that indirectly observes secondary particles produced from galactic cosmic ray air showers[3][4]. The detector element of a neutron monitor consists of a proportional counter containing either ^{3}He or BF_3 gas. In a standard neutron monitor, modeled in Figure 1, the central counter is surrounded by layers of paraffin wax or polyethylene that filters environmental neutrons. A lead producer acts as a target for entering neutrons, enabling nuclear reactions that result in the production of evaporation neutrons, which are then moderated so they might be observed in the proportional counter[5].

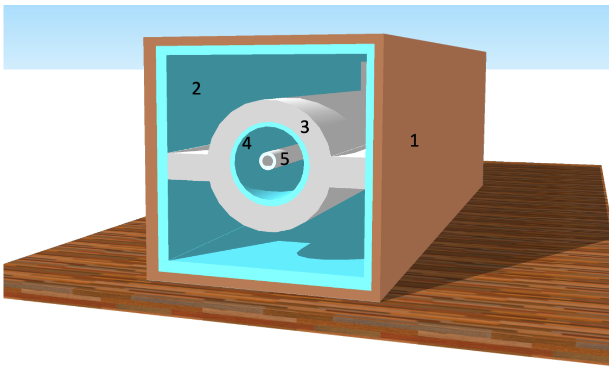

Figure 1: Schematic of a neutron monitor, similar to the configuration at the South Pole. 1) Outer crate housing 2) Polyethylene reflector 3) Lead target producer 4) Polyethylene moderator 5) ^{3}He proportional counter. Additionally, the South Pole Neutron Monitor system is equipped with insulation and heaters.

Worldwide, neutron monitors have been in operation for more than seven decades [6] with a large number of them providing data to the public. A single neutron monitor station gives the integral cosmic ray rate above the local geomagnetic cutoff. By exploiting the array of neutron monitors distributed across latitudes with different geomagnetic cutoffs, spectral and anisotropy studies can be carried out. Neutron monitors provide continuous, real-time data on galactic cosmic ray rates, have observed the past seven solar cycles, and are sensitive to transient events. These include Forbush decreases as well as the ground level enhancement of radiation caused by coronal mass ejections, in which the monitors observe solar energetic particles[7][8][9]. Neutron monitors can provide calibration information for space borne cosmic ray detectors, and can be used as a benchmark for simulations of the production, acceleration, and transport of solar energetic particles.

A specific construction of a neutron monitor is referred to as the NM64 model[4]. In an NM64, the reflector is a thick-walled polyethylene structure. It acts as a filter by rejecting low energy environmental neutrons that are prevalent in the atmosphere, while allowing higher energy neutrons to pass through, as these may be secondaries from cosmic ray showers. Particles that traverse the reflector will reach the producer, a target mass of lead surrounding the other internal components. Inelastic collisions between the incoming neutrons and the heavy lead nuclei produce evaporation neutrons at a rate of A^{γ} where A = 208 for lead and $\gamma \sim 0.7$ for incoming neutrons of a few hundred MeV energy[5]. It is due to this phenomenon that the lead is the main source of neutrons that are detected. Next, particles reach the inner moderator, another layer of polyethylene that will slow down the neutrons to near-thermal energies, ultimately facilitating their capture in the proportional counter. The counter is the central component of the monitors, composed of a steel tube filled with ^{3}He gas. Neutrons are captured in the ^{3}He through the reaction, n + ^{3}He $\rightarrow$ p + ^{3}H + Q, where Q = 764 keV. The full 764 keV is not always available for ionizing the gas as either the proton or triton can collide with the wall of the tube before depositing all of their energy. This leads to the characteristic pulse height distribution of a ^{3}He neutron monitor with a distinct peak that is preceded by two plateaus due to the wall effects.

Figure 2: The 3NM64 system during Auroral activity. The South Pole Station can be seen in the background on the right. Photo Credit NSF/R. Streeter.

The South Pole Station Neutron Monitor [10] is composed of three insulated and heated NM64 model neutron monitors on an elevated outdoor platform (3NM64), shown in Figure 2, as well as twelve “bare” monitors that are housed inside the South Pole Station. Neutron monitors have operated at the South Pole since 1964. The location of the Amundsen-Scott South Pole Station has an elevation of 2800 m, with an essentially atmospheric vertical cutoff of 0.1 GV. Because of the extreme environment, the three NM64’s are installed in individual, insulated housing and are heated to approximately -10°C.

Previously reported observations of apparent neutron bursts from air shower cores impacting the soil near cosmic ray detectors [11][12] opens the question on whether such bursts might be observable for air shower cores impacting the snow and ice near the South Pole Neutron Monitor. In this work, the FLUKA Monte Carlo simulation package is used to investigate a possible background in ground-based observations of neutrons caused by air shower cores penetrating the ice and snow below the exterior 3NM64 system.

2. Simulation

FLUKA [13][14] is a multipurpose Monte Carlo transport code used to simulate particle transport and particle interactions. It can simulate the interaction and propagation of about sixty different particles in complex user-defined geometries with high accuracy. In some cases particles can be simulated up to thousands of TeV in energy and, in the particular case of neutrons, down to thermal energies. FLUKA modeling is optimized at the single particle level through comparison with real data. Flair [15] is an advanced user-friendly graphical interface for FLUKA, which provides an accessible route to constructing FLUKA projects. Flair also provides tools for preliminary analysis of data including graphical analysis.

For this project all relevant processes are activated in FLUKA, including low energy neutron transport, which is key in neutron monitor physics. A simulation of the complete 3NM64 neutron monitor system and environment was constructed. This includes the proportional counter, moderator, lead, reflector, outer housing and platform of the 3NM64, as shown in Figure 3, as well as a model of the South Pole atmospheric density profile composed of eighty-five layers reaching an altitude of 20 km, and a model of the Antarctic ice firn composed of twelve layers of increasing ice density reaching a depth of 180 m.

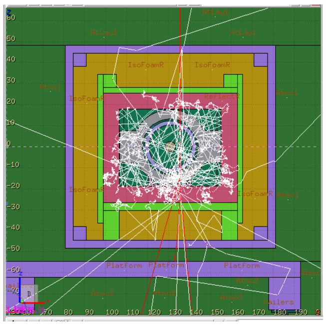

Figure 3: One of the simulated NM64 monitors. Particle tracks in white indicate neutron interactions and transport occurring inside the monitor.

In order to deduce if there is an observable difference in neutron counts due to products of neutron bursts occurring from air shower cores in the snow and ice below the platform, a three step simulation process was executed. Initially, eight energy bins of primary protons extending up to 300 GeV were injected at the top of the simulated atmosphere. At the equivalent atmospheric height of the 3NM64 platform, called observation level, the positions and energy distributions of secondary protons and neutrons were recorded, as shown in Figure 4. This information was then used to determine the initial conditions for the rest of the study.

The second and third simulation steps are identical, except for the simulated environment around the 3NM64 platform. Both begin with protons and neutrons, reaching up to 300 GeV, being re-injected into the atmosphere at observation level according to the previously recorded energy distributions. In the second step the ice is simulated below the platform as usual. This allows air shower cores and already produced secondaries to enter the ice. Some of these particles will then produce more secondaries, which may scatter upward and out of the ice. However, for the third step the ice underlying the 3NM64 is excluded so only neutrons that originate directly from air showers cascading through the atmosphere can be observed. In both scenarios, data was collected on the neutrons that enter the central proportional ^{3}He counter in each of the 3NM64 modules.

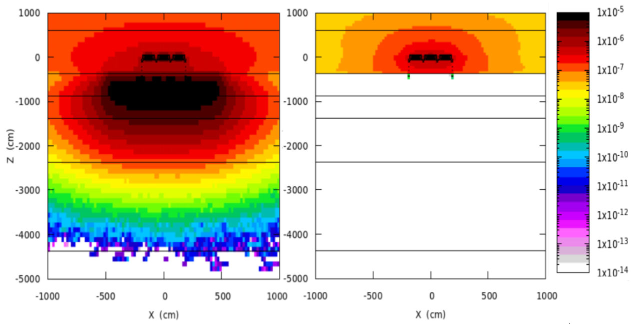

Figure 5: The fluence of secondary neutrons (left) produced in the second step, from air showers in the atmosphere as well as the ice, and (right) produced in third step, where production is only atmospheric.

This process, shown in Figure 5, provides two separate data sets. The first includes both neutrons originating from the initial air shower and products from the ice, whereas the second only includes neutrons originating from the air showers in the atmosphere. Then, the difference between these two data sets can be attributed solely to neutrons that have originated from the ice. There are two likely sources of neutrons that come from the ice and then reach the 3NM64, neutrons from the air shower that scatter upward after reaching the ice and neutrons that are produced within the ice from the proton core of the air shower.

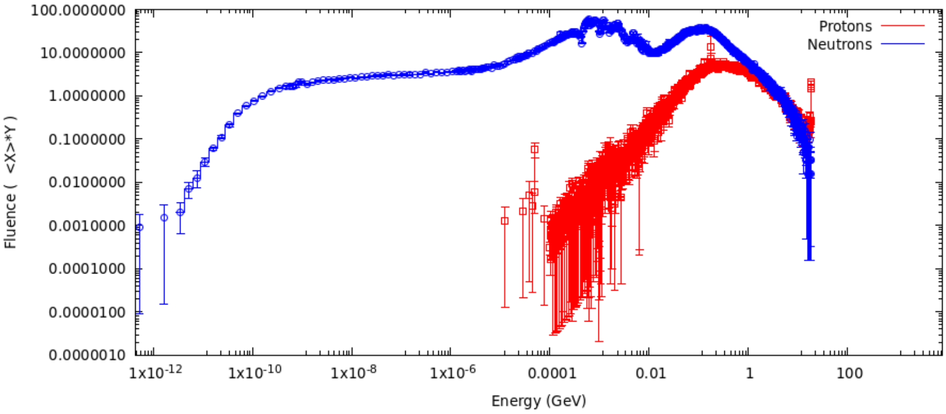

Figure 4: Observed fluence versus energy of secondary neutrons and protons respectively. Here, both are produced from 20 GeV protons injected at the top of the atmosphere. Data was collected at observation level. Fluence is initially measured in $\text{cm}^{-2}\ \text{GeV}^{-1}$ per incident primary unit weight, but presented here as (average bin energy $\times$ fluence) to better resolve features within the spectra.

3. Results and Discussion

When creating the timing distributions of secondary neutrons, it was assumed that the curvature of the shower front can be ignored at the length scale of the neutron monitors since they extend only a few meters in each horizontal direction and primaries were injected vertically above the monitors. Secondary particles re-injected in the 3NM64 simulation were deemed to be injected at time $t = 0$ and the times of all particles are recorded with respect to this time.

All neutrons that entered any of the three ^{3}He tubes were recorded and a distribution of the arrival times of those neutrons is shown in Figure 6. Here, a hint of the neutron burst phenomenon is present in the region past 10 ms, where all of the detected neutrons originate from the simulation including the snow and ice. However, it is a region of limited statistics at these longer times. Figure 7 focuses on a region of higher statistics and shows neutrons that arrive at the detector within 1 ms. It can be seen that there is a larger number of neutron counts from the data that includes the snow and ice in comparison to the data that only includes neutrons from the air shower.

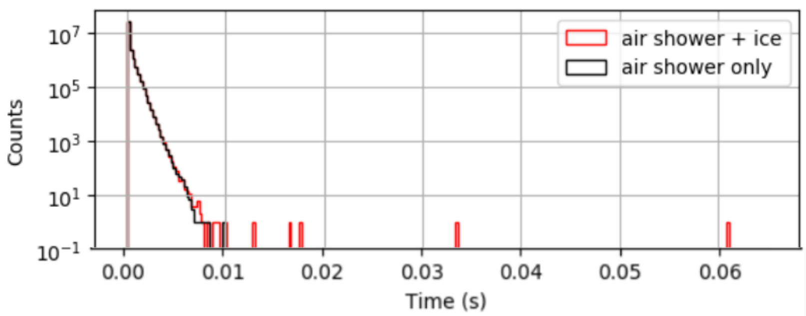

Figure 6: The distribution of arrival times of neutrons in any of the three ^{3}He counters. The red distribution shows neutrons arriving from the air shower as well as those produced from air shower cores that enter the ice. The black curve shows the neutrons arriving only from the initial air shower.

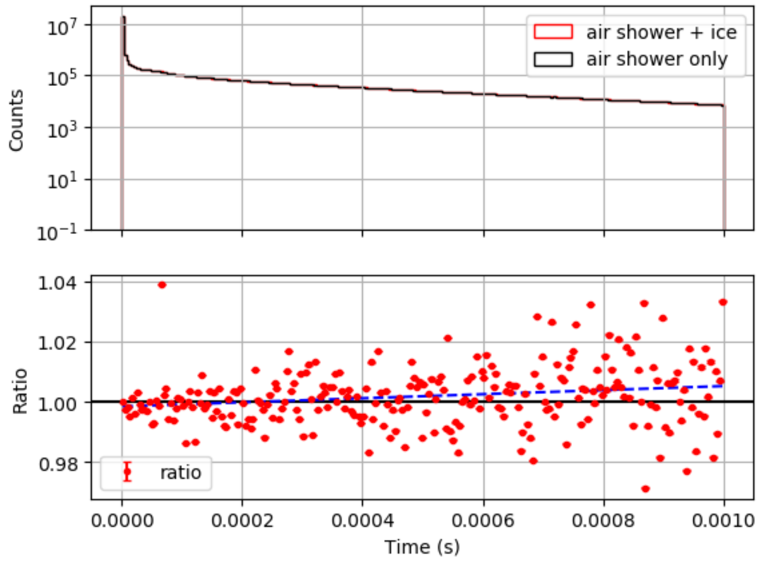

Figure 7: Top: The arrival time distribution similar to Figure 6. Bottom: The ratio of these two distributions. The blue dashed line shows a positive linear correlation in the data signifying that as the time increases, there are more neutrons arriving at the monitors from the atmosphere and ice than neutrons arriving solely from the atmosphere. This hints that even at shorter arrival times, there is neutron production that is occurring in the ice and snow below the monitors that is in excess of the neutrons produced only in the atmosphere.

A neutron monitor is designed to capture thermal neutrons that enter the ^{3}He. Figures 8 and 9 show results for thermal neutrons only. Again, all the thermal neutrons that arrive in the monitors after 10 ms are originating from the snow and ice simulation. This is another hint of neutron bursts occurring in the snow, however it is another region of limited statistics.

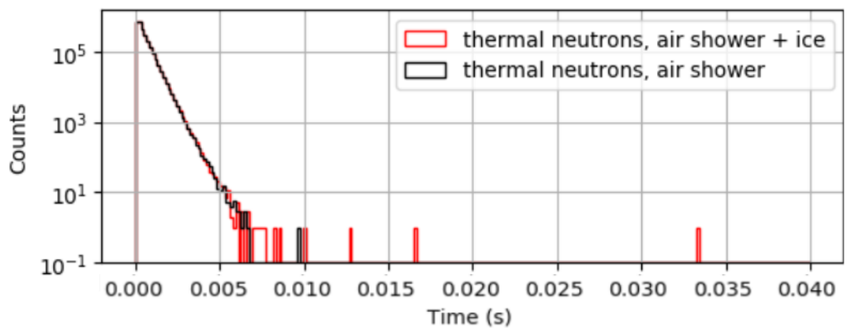

Figure 8: Same as Figure 6 but with only thermal neutrons included. The threshold energy for thermal neutrons was found to be around 0.034eV using the rms value from the Maxwell-Boltzmann distribution, and accounting for the fact that the 3NM64 is heated to roughly -10°C at the South Pole.

Throughout this study we observe a possible hint of neutron bursts originating from air shower cores that enter into the ice below the neutron monitor platform. At longer times, specifically in the region from 10 ms to over 60 ms, all of the observed counts are from the data collected when particles in the simulation are allowed to enter the ice below the platform. This hints that these long

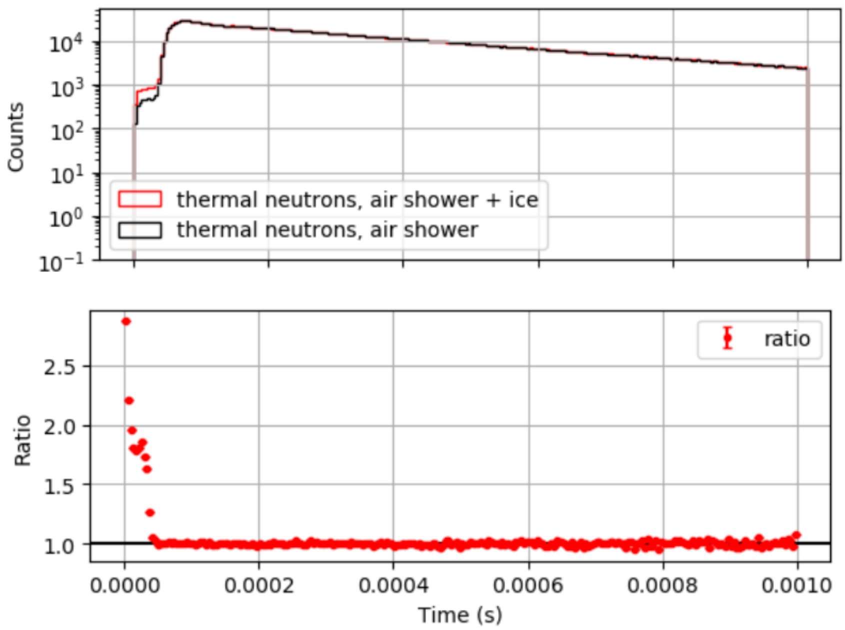

Figure 9: Top: The arrival time distribution similar to Figure 8. Bottom: The ratio of these two distributions. An increased number of counts from the snow can be seen preceding 0.1ms at thermal energies. While this is an interesting feature, this region is within the neutron monitor dead time so the excess is cannot be observed.

duration counts are originating in the ice, rather than in the air shower that occurs in atmosphere. However, there are limited statistics in the region above 10 ms. There are a few reasons that this phenomenon may not be overwhelmingly present in this work. First, given that the ice below the neutron monitors act as a moderator, neutrons produced in the ice may undergo more than enough scatterings, roughly 200 or so, and be moderated down to thermal energies before they escape the ice, if at all. Ultimately, this may mean that the neutrons do not have enough energy to enter the monitor. Second, the highest energy primaries used in this study are 300 GeV, perhaps too low to observe a strong impact from the neutron bursts. More work must be done to determine if neutron bursts significantly impact spectral studies at the South Pole. This follow up work may include exploring neutrons from higher energy shower cores, as well as the potential for other particle species to initiate the neutron bursts in the ice.

4. Acknowledgment

This work is supported by the National Science Foundation awards: Collaborative Research: The Simpson Neutron Monitor Network, Award Number: 2112437 and ANSWERS: Understanding and Forecasting Solar Energetic Particles in the Inner Solar System and Earth's Magnetosphere, Award Number: 2149771 (UWRF Sub-Award). Chloe Heifner is partially supported by UWRF's office of Undergraduate Research, Scholarly, and Creative Activity. We thank Pierre-Simon Mangeard for advice on simulating the South Pole atmosphere with FLUKA and Waraporn Nyntiyakul's research group for invaluable help with FLUKA simulations.

References

[1] V.F. Hess. *Über Beobachtungen der durchdringenden Strahlung bei sieben Freiballonfahrten*. *Phys. Z.*, **13**:1084–1091, (1912).

[2] R. Engel, D. Heck, and T. Pierog. *Extensive Air Showers and Hadronic Interactions at High Energy*. *Annu. Rev. Nucl. Part. S.*, **61**(1):467–489, (2011).

[3] J.A. Simpson. *The Cosmic Ray Nucleonic Component: The Invention and Scientific Uses of the Neutron Monitor*. *Space Sci. Rev.*, **93**:11–32, (2000).

[4] C.J. Hatton and H. Carmichael. *Experimental Investigation of the NM-64 Neutron Monitor*. *Can. J. Phys.*, **42**(12):2443–2472, (1964).

[5] P.H. Stoker, L.I. Dorman, and J.M. Clem. *Neutron Monitor Design Improvements*. *Space Sci. Rev.*, **93**:361–380, (2000).

[6] P. Väisänen, I. Usoskin, and K. Mursula. *Seven Decades of Neutron Monitors (1951-2019): Overview and Evaluation of Data Sources*. *J. Geophys. Res. Space Phys.*, **126**:5, (2021).

[7] J. W. Bieber, J. Clem, P. Evenson, R. Pyle, A. Sáiz, and D. Ruffolo. *Giant Ground Level Enhancement of Relativistic Solar Protons on 2005 January 20. I. Spaceship Earth Observations*. *Astrophys. J.*, **771**(2):92, (2013).

[8] J.A. Lockwood. *Forbush Decreases in the Cosmic Radiation*. *Space Sci. Rev.*, **12**(5):658–715, (1971).

[9] A. Mishev and I. Usoskin. *Current Status and Possible Extension of the Global Neutron Monitor Network*. *J. Space Weather Space Clim.*, **10**:17, (2020).

[10] J. Clem P. Evenson, J. Bieber and R. Pyle. *South Pole Neutron Monitor Lives Again*. In proceedings of the *32nd International Cosmic Ray Conference, ICRC 2011*, Beijing (2011).

[11] G.S. Bowers et. al. *Fair Weather Neutron Bursts From Photonuclear Reactions by Extensive Air Shower Core Interactions in the Ground and Implications for Terrestrial Gamma ray Flash Signatures*. *Geophys. Res. Lett.*, **48**:6, (2021).

[12] Yu.V. Stenkin, J.F. Valdés-Galicia, A. Hurtado, and O. Musalem. *Study of "neutron bursts" with Mexico City neutron monitor*. *Astropart. Phys.*, **16**(2):157–168, (2001).

[13] C. Ahdida et. al. *New Capabilities of the FLUKA Multi-Purpose Code*. *Front. Phys.*, **9**:788253, (2022).

[14] G. Battistoni et. al. *Overview of the FLUKA code*. *Annals Nucl. Energy*, **82**:10–18, (2015).

[15] V. Vlachoudis. *Flair: A powerful but user friendly graphical interface for FLUKA*. In proceedings of the *International Conference on Mathematics, Computational Methods & Reactor Physics 2009*, Saratoga Springs, New York (2009).